

# Errors due to Finite Rise/fall Times of Pulses in Superconducting Charge Qubits

Sangchul Oh<sup>1,\*</sup>

<sup>1</sup>*Department of Physics, Korea Advanced Institute of Science Technology, Daejeon 305-701, Korea*  
(Dated: November 20, 2018)

We study numerically the dynamics of two-qubit gates with superconducting charge qubits. The exact ratio of  $E_J$  to  $E_L$  and the corresponding operation time are calculated in order to implement two-qubit gates. We investigate the effect of finite rise/fall times of pulses in realization of two-qubit gates. It is found that the error in implementing two-qubit gates grows quadratically in rise/fall times of pulses.

PACS numbers: 03.67.Lx, 73.23.-b, 85.25.Cp

## I. INTRODUCTION

Building a practical quantum computer with a large number of qubits has recently attracted much attention since the useful quantum algorithms<sup>1,2</sup> and the quantum error-correction codes<sup>3,4</sup> were developed. Basic quantum logic gates were implemented on trapped ions<sup>5,6</sup>, QED cavities<sup>7</sup>, and liquid state NMR<sup>8,9,10</sup>. Solid-state devices have advantages of large scale integration, flexibility in the design, and easy connection to conventional electronic devices. Some of solid-state devices proposed are as follows: electron spins in quantum dots<sup>11</sup>, nuclear spins of donor atom in silicon<sup>12</sup>, and ultrasmall Josephson junctions<sup>13,14,15,16,17,18</sup>.

Two types of superconducting qubits based on ultrasmall Josephson junctions were proposed. One is to use a number of excess Cooper pairs on a superconducting Cooper-pair box, called the superconducting charge qubit<sup>14,15,16</sup>. And the other is to utilize a single flux quantum of a superconducting loop, called the superconducting flux qubit<sup>13</sup>. Here, we focus on superconducting charge qubits. In theoretical aspects, the measurement of superconducting charge states using a single electron transistor and decoherence due to coupling of qubits with environments were studied<sup>17,18</sup>. Also the quantum leakage of superconducting charge qubits was pointed out<sup>19</sup>. In experiments, Nakamura *et al.*<sup>20</sup> demonstrated the coherent oscillations of Cooper pairs on a superconducting Cooper-pair box. This corresponds to a rotation of a single qubit about  $x$  axis. Thus the realization of two-qubit gates is an important step for making a superconducting quantum computer with a medium size.

In this paper, we investigate how the two-qubit gate could be implemented on superconducting charge qubits. The pulse sequence and operation times, and the simulation of two-qubit gates are reported. We examine errors due to finite rise/fall times of pulses in the realization of two-qubit gates.

Our paper is organized as follows. In Sec. II we introduce the Hamiltonians of superconducting charge qubits and of ideal qubits. A numerical method which allows us to simulate a quantum computer is presented. In Sec. III we explicitly show the pulse sequence necessary to implement two-qubit gates with superconducting charge

qubits. Also numerical studies of two-qubit gates are presented. In Sec. IV we analyze errors due to finite rise/fall times of pulses on superconducting charge qubits. Finally, in Sec. V we summarize the results.

## II. HAMILTONIAN OF SUPERCONDUCTING CHARGE QUBITS

In this paper we consider two qubit systems: ideal qubits and superconducting charge qubits<sup>16,18</sup>. By comparing two qubit systems, one can discover differences and similarities between them, which will be helpful to improve the design of superconducting charge qubits.

First consider an ideal model for a quantum computer. The Hamiltonian of the system of  $N$  ideal qubits reads

$$H_q^{\text{ideal}}(t) = -\sum_{i=1}^N \mathbf{B}_i(t) \cdot \boldsymbol{\sigma}^{(i)} - \frac{1}{2} \sum_{i<j} J_{ij}(t) [\sigma_x^{(i)} \sigma_x^{(j)} + \sigma_y^{(i)} \sigma_y^{(j)}], \quad (1)$$

where  $\boldsymbol{\sigma}^{(i)} = (\sigma_x^{(i)}, \sigma_y^{(i)}, \sigma_z^{(i)})$  are Pauli matrices for the  $i$ -th qubit. Here the Zeeman coupling terms  $\mathbf{B}_i(t)$  and the inter qubit couplings  $J_{ij}(t)$  can be turned on and off between zero and finite values in a controlled way.

Let us consider a system of  $N$  superconducting charge qubits<sup>14,16,18</sup>. Each qubit consists of a single-Cooper-pair box with two ultrasmall Josephson junctions of capacitance  $C_J^0$  forming a DC-SQUID ring and a gate electrode with capacitance  $C_g$ . The dynamics of a qubit is characterized by relevant energy scales; superconducting gap  $\Delta$ , charging energy  $E_C \equiv e^2/2(C_g + 2C_J^0)$ , Josephson coupling energy  $E_J^0$ , and thermal fluctuation  $k_B T$ . Assume that the system is in the regime of  $E_C \ll \Delta$  and  $k_B T \ll E_C$  in order to suppress quasi-particle tunneling or excitation. Also suppose that the system operates under the conditions  $E_J \ll E_C$  and  $C_g V_g / (2e) \sim 1$ . Then only two charge states  $\{|0\rangle, |1\rangle\}$ , no excess Cooper pair and one excess Cooper pair on the box, play a role and represent the qubit. A few ways of coupling charge qubits were proposed<sup>14,15,16,18</sup>. Here we consider the coupling between charge qubits via the  $LC$  resonant circuit, where

$N$  charge qubits are connected in parallel to a common inductor with inductance  $L$ . The Hamiltonian of the system of  $N$  superconducting charge qubits is given by

$$H_q(t) = -\frac{1}{2} \sum_{i=1}^N [E_{C_i} \sigma_z^{(i)} + E_{J_i}(\Phi_{X_i}) \sigma_x^{(i)}] - \sum_{i \neq j} \frac{E_{J_i} E_{J_j}}{E_L} \sigma_y^{(i)} \sigma_y^{(j)}, \quad (2)$$

where  $E_{C_i} = 4E_C(C_{g_i}V_{g_i}/e - 1)$  is turn on and off by applying the gate voltage  $V_{g_i}$  on the  $i$ -th gate electrode. Here  $E_{J_i}(\Phi_{X_i}) = 2E_J^0 \cos(\pi\Phi_{X_i}/\Phi_0)$  is the effective Josephson energy of the  $i$ -th qubit, and controlled by the external flux  $\Phi_{X_i}$ .  $\Phi_0 = \hbar/2e$  is a flux quantum. Here is  $E_L = \frac{\Phi_0^2}{\pi^2 L} (2C_J^0/C_{qb})^2$  with  $C_{qb}^{-1} = (2C_J^0)^{-1} + C_g^{-1}$ .

The Hamiltonian of Eq. (2) is similar to the ideal one of Eq. (1) except one fact. The system of superconducting charge qubits has only two kinds of independently controllable parameters,  $\{E_{C_i}, E_{J_i}\}$ , whereas the ideal model has four kinds of controllable parameters  $\{B_{x_i}, B_{y_i}, B_{z_i}, J_{ij}\}$ . Coupling between two superconducting charge qubits could be realized by turning on both  $E_{J_i}$  and  $E_{J_j}$ . This causes somewhat disadvantages in operating two-qubit gates, which will be discussed in Sec. IV.

The time-evolution of  $N$  qubits is governed by a time-dependent Schrödinger equation

$$i\hbar \frac{\partial}{\partial t} |\psi\rangle = H_q(t) |\psi\rangle, \quad (3)$$

where  $|\psi\rangle = \sum_{m=0}^L a_m(t) |m\rangle$  with  $L \equiv 2^N - 1$  and  $a_m \in \mathbf{C}$ . Its computational basis is represented by a tensor product of individual qubits,  $|m\rangle = |q_1\rangle \otimes |q_2\rangle \otimes \cdots \otimes |q_N\rangle$ , where integer  $m = 2^{N-1}q_1 + 2^{N-2}q_2 + \cdots + 2^0q_N$  and  $q_i \in \{0, 1\}$ . Multiplying both sides of Eq. (3) by  $\langle n|$ , one gets a set of  $N$  coupled first-order ordinary differential equations for the function  $a_n(t)$

$$\dot{a}_n = -\frac{i}{\hbar} \sum_{m=0}^L H_{nm}(t) a_m, \quad (4)$$

where  $H_{nm}(t) \equiv \langle n| H_q(t) |m\rangle$ . We developed a program which allows us to solve the above initial value problem and to simulate a quantum computer. Our code is based on the Runge-Kutta method<sup>22</sup>.

A quantum logic gate can be realized by controlling the time-evolution operator which acts on selected qubits for a fixed period of time. A way to control the time-evolution operator is to turn on or off each terms in the Hamiltonians of Eq. (1) or (2). For an example, a pulse  $P(t)$ , which is applied as  $B_{\alpha i}(t) = B_{\alpha i}^0 P(t)$  with  $\alpha = x, y, z$ , makes it possible to change a term of the Hamiltonian from zero to finite value  $B_{\alpha i}^0$  for a finite time  $\tau$ . In this paper, we consider a rectangular pulse  $P_{\text{rec}}(t)$  with width  $\tau = t_b - t_a$  and a unit height, modeled

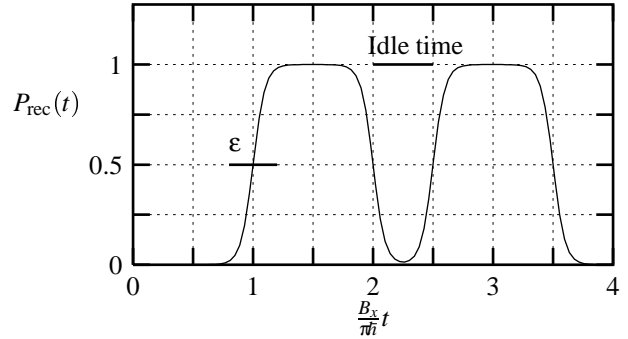


FIG. 1: Rectangular pulses with finite rise/fall time  $2\epsilon$  are plotted as a function of time. Here time is normalized in the unit of  $\pi\hbar/B_x$ . The role of idle time between two successive pulses is to prevent the tails of pulses from overlapping each others.

by a kink and anti-kink pair

$$P_{\text{rec}}(t) = \frac{1}{2} \left[ \tanh\left(\frac{t-t_a}{\epsilon/2}\right) + \tanh\left(\frac{t_b-t}{\epsilon/2}\right) \right], \quad (5)$$

where the rise (or fall) time is about  $2\epsilon$ . That means  $P_{\text{rec}}(t_a + \epsilon) \gtrsim \tanh(2) \approx 0.964$  for  $\tau > 2\epsilon$ . The smaller  $\epsilon$  one takes, the sharper rectangular pulse one obtains. Fig. 1 illustrates a sequence of two rectangular pulses.

### III. CNOT GATE WITH SUPERCONDUCTING CHARGE QUBITS

In this section, we explicitly show how the controlled-not (CNOT) gate with superconducting charge qubits could be implemented by applying a sequence of pulses. What makes the CNOT gate so important is that the CNOT gate (or any nontrivial two-qubit gate) and single-qubit gates form a universal set of logic operation. Also a general two-qubit controlled- $U$  gate can be built up of two CNOT gates and three single-qubit gates. The CNOT gate acting on two qubits  $i$  and  $j$  is represented by the unitary matrix in the basis of  $\{|0_i 0_j\rangle, |0_i 1_j\rangle, |1_i 0_j\rangle, |1_i 1_j\rangle\}$

$$U_{\text{CNOT}}^{ij} = \begin{pmatrix} 1 & 0 & 0 & 0 \\ 0 & 1 & 0 & 0 \\ 0 & 0 & 0 & 1 \\ 0 & 0 & 1 & 0 \end{pmatrix}, \quad (6)$$

where  $i$  and  $j$  are indices for a control bit and a target bit, respectively.

#### A. CNOT gate with ideal qubits

First consider the implementation of the CNOT gate for an ideal system whose Hamiltonian is given by Eq. (1). The primary two-qubit gate acting on the  $i$ -th and  $j$ -th qubits could be implemented by turning

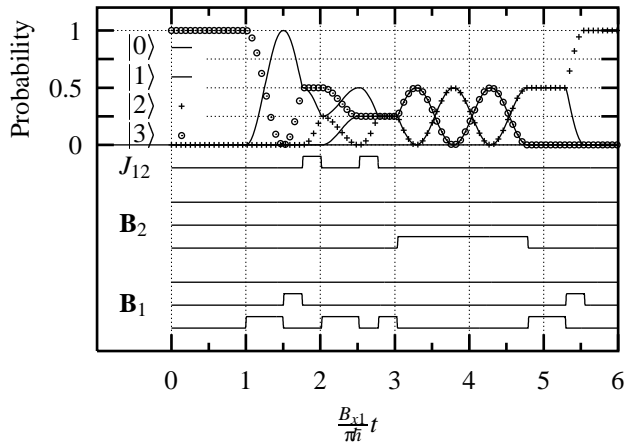


FIG. 2: Time-dependence of probabilities  $|a_{ij}|^2$ 's as a function of the normalized time  $B_{x1}t/\pi\hbar$  on the action of the CNOT gate  $U_{\text{CNOT}}^{12}$  in an ideal model. The sequence of rectangular pulses is given in the below part. Here is  $\mathbf{B}_i = (B_{xi}, B_{yi}, B_{zi})$  with  $i = 1, 2$ .

on the coupling  $J_{ij}(t)$ . It can be written in the basis  $\{|0_i0_j\rangle, |0_i1_j\rangle, |1_i0_j\rangle, |1_i1_j\rangle\}$  as

$$U_{2b}^{ij}(\gamma) = \begin{pmatrix} 1 & 0 & 0 & 0 \\ 0 & \cos \gamma & i \sin \gamma & 0 \\ 0 & i \sin \gamma & \cos \gamma & 0 \\ 0 & 0 & 0 & 1 \end{pmatrix}, \quad (7)$$

where  $\gamma \equiv J_{ij}t/\hbar$ . Then, the CNOT gate for an ideal qubit system can be realized by combining single-qubit gates and the primary two-qubit gate  $U_{2b}^{ij}$

$$U_{\text{CNOT}}^{ij} = H_i e^{i\frac{\pi}{4}} e^{-i\frac{\pi}{4}\sigma_x^{(j)}} e^{i\frac{\pi}{4}\sigma_x^{(i)}} \times U_{2b}^{ij}(\frac{\pi}{4}) e^{i\frac{\pi}{2}\sigma_x^{(i)}} U_{2b}^{ij}(\frac{\pi}{4}) H_i, \quad (8)$$

where  $H_i$  is a Hadamard gate acting on the  $i$ -th qubit.

Fig. 2 depicts the time-evolution of qubits under the action of CNOT gate for the ideal model. The lower part of Fig. (2) illustrates the sequence of rectangular pulses which generates the CNOT gate of Eq. (8). Here is taken  $|\psi_{\text{in}}\rangle = |3\rangle = |11\rangle$ , i.e.,  $|a_{11}|^2 = 1$ , as an initial state (denoted by  $\circ$ ). After implementing the CNOT gate, one obtains  $|a_{10}|^2 = 1$ , corresponding to state  $|10\rangle$ , labeled by  $+$ . In Fig. 2, it takes a long time to implement the single-qubit gate  $e^{-i\frac{\pi}{4}\sigma_x^{(j)}}$  because  $B_{\alpha i}$ 's are taken to be always positive or zero.

## B. CNOT gate with superconducting charge qubits

Let us consider the implementation of the CNOT gate with superconducting charge qubits. The coupling between the  $i$ -th and  $j$ -th qubits can be switched on by turning on Josephson couplings,  $E_{Ji}$  and  $E_{Jj}$ , and by turning off charging energy terms,  $E_{Ci} = E_{Cj} = 0$ . Then, the interaction Hamiltonian between two charge

qubits, for an example qubits 1 and 2, can be written as

$$H_{\text{ph}} = -\frac{E_J}{2}\sigma_x^{(1)} - \frac{E_J}{2}\sigma_x^{(2)} - E_{\text{int}}\sigma_y^{(1)}\sigma_y^{(2)}, \quad (9)$$

where  $E_{\text{int}} \equiv E_J^2/E_L$  with an assumption of  $E_{J1} = E_{J2} \equiv E_J$ . For a moment, suppose that switching  $E_{Ji}$ 's on and off could be done instantaneously. As will be discussed later, a finite time in switching on  $E_{Ji}$ 's gives rise to an error in implementing two-qubit gates.

The basic two-qubit gate is given by the time-evolution operator under the Hamiltonian of Eq. (9) for a finite time  $\tau$

$$U_{\text{ph}}(\tau) = e^{-iH_{\text{ph}}\tau/\hbar}. \quad (10)$$

Let us transform the above time-evolution operator under the unitary operator  $R_y \equiv \exp[-i\frac{\pi}{4}(\sigma_y^{(1)} + \sigma_y^{(2)})]$  as

$$U'_{\text{ph}} \equiv R_y^\dagger U_{\text{ph}} R_y = e^{-iH'_{\text{ph}}\tau/\hbar}, \quad (11)$$

where the Hamiltonian transformed,  $H'_{\text{ph}} \equiv R_y^\dagger H_{\text{ph}} R_y$  reads

$$H'_{\text{ph}} = -\frac{E_J}{2}\sigma_z^{(1)} - \frac{E_J}{2}\sigma_z^{(2)} - E_{\text{int}}\sigma_y^{(1)}\sigma_y^{(2)} \quad (12a)$$

$$= -E_{\text{int}} \begin{pmatrix} a & 0 & 0 & -1 \\ 0 & 0 & 1 & 0 \\ 0 & 1 & 0 & 0 \\ -1 & 0 & 0 & -a \end{pmatrix}. \quad (12b)$$

Here  $a \equiv E_J/E_{\text{int}} = E_L/E_J$ . Note that the Hamiltonian of Eq. (12) does not mix the subspace spanned by  $|00\rangle$  and  $|11\rangle$  with that by  $|01\rangle$  and  $|10\rangle$ . Then the time-evolution operator of the transformed Hamiltonian  $H'_{\text{ph}}$  becomes

$$U'_{\text{ph}} = \begin{pmatrix} \cos \theta + n_z \sin \theta & 0 & 0 & -in_x \sin \theta \\ 0 & \cos \phi & i \sin \phi & 0 \\ 0 & i \sin \phi & \cos \phi & 0 \\ -in_x \sin \theta & 0 & 0 & \cos \theta - n_z \sin \theta \end{pmatrix}, \quad (13)$$

where the time evolution corresponds to the rotation about the  $y$ -axis by angle  $\phi \equiv E_{\text{int}}\tau/\hbar$  in the subspace spanned by  $|01\rangle$  and  $|10\rangle$ . Also in the subspace spanned by  $|00\rangle$  and  $|11\rangle$ , the time evolution gives rise to the rotation about the axis  $(n_x, 0, n_z)$  by angle  $\theta \equiv \sqrt{1+a^2} E_{\text{int}}\tau/\hbar$ , where

$$n_z \equiv \frac{a}{\sqrt{a^2+1}} = \frac{E_L}{\sqrt{E_L^2 + E_J^2}}, \quad (14a)$$

$$n_x \equiv \frac{1}{\sqrt{a^2+1}} = \frac{E_J}{\sqrt{E_L^2 + E_J^2}}. \quad (14b)$$

By choosing the appropriate values  $E_L$ ,  $E_J$ , and  $\tau$ , one can control the rotation angles  $\phi$  and  $\theta$ . Let us consider special angles  $\phi = \frac{\pi}{4}(2m-1)$  with  $m = 1, 2, \dots$ , and  $\theta = n\pi$  with  $n = 0, \pm 1, \pm 2, \dots$ . Note that the case of even  $n$

is same to that of odd  $n$  up to the global phase  $e^{i\pi}$ . These angles can be obtained by taking the evolution-time  $\tau = \frac{\pi}{4}(2m-1)\frac{\hbar}{E_{\text{int}}}$ , which is given by the relation of angle  $\phi$ . Then one has  $\theta = \frac{\pi}{4}(2m-1)\sqrt{1+a^2} = \frac{\pi}{4}\sqrt{1+E_L^2/E_J^2} = n\pi$ . Thus we obtain the relation between  $E_L$  and  $E_J$

$$\frac{E_L}{E_J} = \sqrt{\left(\frac{4n}{2m-1}\right)^2 - 1}, \quad (15)$$

where it could be accomplished by tuning  $E_J$  or  $E_L$ . Note that one can not take  $n = 0$ . Also the evolution-time is given by

$$\tau = \frac{\pi\hbar}{4E_J} \sqrt{(4n)^2 - (2m-1)^2}. \quad (16)$$

We have the basic two-qubit gate  $U_{\text{ph}} = R_y U'_{\text{ph}} R_y^\dagger$  written by

$$U_{\text{ph}} = \frac{1}{2} \begin{pmatrix} 1 + e^{i\phi} & 0 & 0 & 1 - e^{i\phi} \\ 0 & 1 + e^{-i\phi} & 1 - e^{-i\phi} & 0 \\ 0 & 1 - e^{-i\phi} & 1 + e^{-i\phi} & 0 \\ 1 - e^{i\phi} & 0 & 0 & 1 + e^{i\phi} \end{pmatrix}, \quad (17)$$

where  $\phi = \frac{\pi}{4}(2m-1)$  with  $m = 1, 2, \dots$ . By combining  $U_{\text{ph}}$  with single-qubit gates, the controlled phase flip gate  $U_{\text{CPF}}^{ij}$ , operating on the  $i$ -th and  $j$ -th qubits, can be realized by

$$U_{\text{CPF}}^{ij} = e^{-i\phi\sigma_z^{(i)}} e^{i\phi\sigma_z^{(j)}} U_{\text{ph}}^{ij} e^{-i\pi\sigma_z^{(i)}/2} U_{\text{ph}}^{ij}, \quad (18)$$

where  $\phi$  is the value given above. By using the controlled phase flip gate  $U_{\text{CPF}}^{ij}$  and the Hadamard gate  $H_j$  on qubit  $j$ , the CNOT gate can be implemented by

$$U_{\text{CNOT}}^{ij} = H_j U_{\text{CPF}}^{ij} H_j. \quad (19)$$

Taking  $m = 1$  and  $n = 3$ , one gets  $E_L = \sqrt{143}E_J$ . This value satisfies the physical condition  $E_L \sim 10E_J$ <sup>16,18,21</sup>. The typical time-scale for operating the basic two-qubit gate is given by  $\tau = \frac{\pi\hbar}{4E_J}\sqrt{143}$ , which is much longer than the operation time of the single-qubit gate,  $\tau_{\text{op}} = \hbar/E_J$  or  $\hbar/E_{Ci}$ . Fig. 3 shows time-evolution of qubits when  $|\psi_{\text{in}}\rangle = |11\rangle$  is taken as an input (denoted by  $\circ$ ). After operating the CNOT gate on two qubits, one gets the output  $|\psi_{\text{out}}\rangle = |10\rangle$ , which is labeled by  $\times$ .

#### IV. ERRORS DUE TO FINITE RISE/FALL TIMES OF PULSES

Up to now, it was assumed that the effective Josephson coupling  $E_{Ji}(t)$  could be switched on (or off) instantaneously. This means a pulse applied is a perfect rectangular one and has no rise/fall times. However, in reality it takes finite times to turn on (or off) pulses fully. While  $E_{Ji}(t)$ 's being switched on (or off), the Hamiltonian of Eq. (9)  $H_{\text{ph}}$  becomes time-dependent and the  $H_{\text{ph}}$ 's at different times do not commute, i.e.,

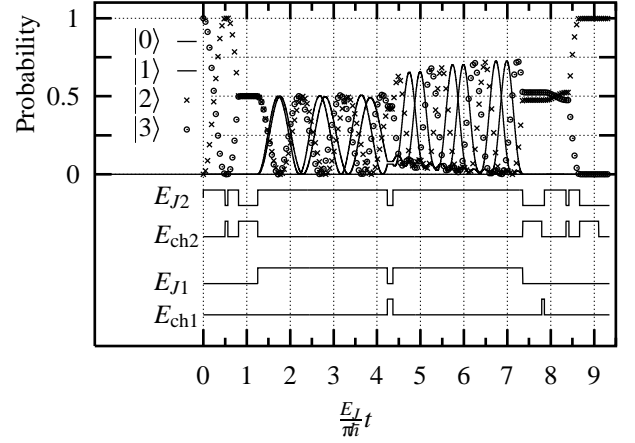


FIG. 3: Time-evolution of probabilities of qubits as a function of time on action of the CNOT gate for superconducting charge qubits. Time is normalized in the unit of  $\pi\hbar/E_J$ .  $E_{Ci}/E_J = 2$  and  $E_L = \sqrt{143}E_J$  are taken. The sequence of rectangular pulses is depicted in the below.

$[H_{\text{ph}}(t), H_{\text{ph}}(t')] \neq 0$  for  $t \neq t'$ . This causes an error in the realization of two-qubit gates with superconducting charge qubits. If Hamiltonian's at different times commute, the shape of the pulse applied is of no importance. The ideal qubits and single-qubit rotations of superconducting charge qubits are free from this problem.

The Magnus expansion<sup>23</sup> provides the means of representing the time-evolution operator of a time-dependent Hamiltonian  $H(t)$  as

$$U(t) = T e^{-\frac{i}{\hbar} \int_0^t d\tau H(\tau)} = e^{-\frac{i}{\hbar} \bar{H} t}, \quad (20a)$$

where  $T$  denotes the time-ordering operator. Here the average Hamiltonian is given by  $\bar{H} = \bar{H}^{(0)} + \bar{H}^{(1)} + \dots$  where

$$\bar{H}^{(0)} = \frac{1}{\tau} \int_0^\tau dt_1 H(t_1), \quad (20b)$$

$$\bar{H}^{(1)} = \frac{-i}{2\tau\hbar} \int_0^\tau dt_2 \int_0^{t_2} dt_1 [H(t_2), H(t_1)]. \quad (20c)$$

If the rise/fall time is short, then the approximation to the first term  $\bar{H}^{(0)}$  is good. Otherwise the higher order terms become significant. If the pulse for the rise time is modeled by  $P(t) = t/2\epsilon$ , the first term  $\bar{H}^{(1)}$ , which arises when the basic two-qubit gate  $U_{\text{ph}}$  is implemented, can be written by

$$\bar{H}^{(1)} \approx -\frac{E_J^3 \epsilon}{15E_L \hbar} \left( \sigma_z^{(1)} \sigma_y^{(2)} + \sigma_y^{(1)} \sigma_z^{(2)} \right). \quad (21)$$

The error due to the finite rise/fall times of pulses is quantified by the gate fidelity<sup>24</sup>

$$F = \langle \psi_{\text{in}} | U^\dagger \rho_{\text{out}} U | \psi_{\text{in}} \rangle = |\langle \psi_{\text{out}} | \psi_{\text{out}}^\epsilon \rangle|^2, \quad (22)$$

where  $U$  is the unitary operator corresponding to the ideal gate when perfect rectangular pulses are applied.

On the other hand, the unitary operator generated by pulses with finite rise/fall times transforms the input state  $|\psi_{\text{in}}\rangle$  into the density operator of the imperfect output state  $\rho_{\text{out}}$ . In our case the gate fidelity is nothing but the square of the overlap between the perfect output state  $|\psi_{\text{out}}\rangle = U|\psi_{\text{in}}\rangle$  and the imperfect output state  $\rho_{\text{out}} = |\psi_{\text{out}}^\epsilon\rangle\langle\psi_{\text{out}}^\epsilon|$ . Assuming that Eq. (21) is small, it is straightforward to calculate the gate fidelity

$$F \approx |\langle\psi_{\text{in}}|e^{-i\bar{H}^{(1)}\tau/\hbar}|\psi_{\text{in}}\rangle|^2 \approx 1 - \epsilon^2\langle\Delta\eta^2\rangle \quad (23)$$

where  $\langle\Delta\eta^2\rangle \equiv \langle\psi_{\text{in}}|\eta^2|\psi_{\text{in}}\rangle - (\langle\psi_{\text{in}}|\eta|\psi_{\text{in}}\rangle)^2$  is the dispersion of  $\eta \equiv \bar{H}^{(1)}\tau/\hbar\epsilon$ . For small rise/fall time, error grows quadratically in rise/fall time  $2\epsilon$ .

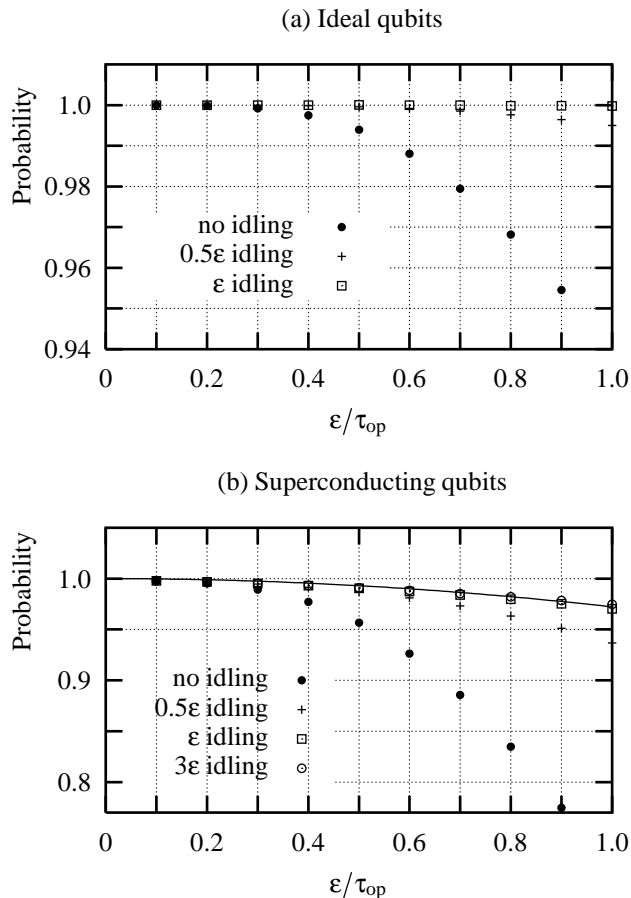


FIG. 4: Probability of success on the action of the CNOT gate as a function of the ratio of the rise/fall time to the operation time,  $\epsilon/\tau_{\text{op}}$ : (a) ideal qubits (b) superconducting charge qubits. Here the time scale of operation is  $\tau_{\text{op}} = \hbar/B_z$  for the ideal case and  $\tau_{\text{op}} = \hbar/E_{C_i}$  for the superconducting case. Idle times prevent the tails of pulses from overlapping. The solid line is the fitting function  $1 - 0.027(\epsilon/\tau_{\text{op}})^2$  which shows the quadratic growth of error in rise/fall times.

Fig. 4 shows the numerical study of the error due to finite rise/fall times in implementing the CNOT gate with superconducting charge qubits. For ideal qubits, if finite idle times between successive pulses are applied, the correct CNOT gate is realized. However, for superconducting charge qubits, although a finite idle time reduces the error, there still exists the error due to finite rise/fall times. As shown in Fig. 4 (b), the probability of getting the correct state reduces quadratically in rise/fall time  $2\epsilon$  in agreement with the theoretical prediction of Eq. (23).

In Nakamura *et al.*'s experiment<sup>20</sup>, the rise/fall times of the pulse was about 30 – 40 ps at the top of the cryostat. If the effective Josephson coupling is  $E_J \approx 50 \mu\text{eV}$ , then the timescale of single-qubit  $x$  rotation is about  $\hbar/E_J \approx 1$  ps. This means that the rise/fall times of the pulses should be less than 1 ps in order for two-qubit gates to be implemented correctly. It should be noted that this type of errors is caused by the coupling scheme between two qubits. Thus this problems can be solved by improving the design of devices, i.e., by introducing new ways of two-qubit couplings.

## V. SUMMARY

We have studied the dynamics of qubits on the action of CNOT gates for ideal and superconducting charge qubits. We have explicitly shown how the CNOT gate could be implemented for superconducting charge qubits. It is found that the error in implementing two-qubit gates with superconducting charge qubits grows quadratically in finite rise/fall times. Thus it is necessary to keep the rise/fall times small or to find new ways of coupling two qubits other than the coupling scheme via the common inductor.

## Acknowledgments

The author would like to thanks Y. Makhlin, A. Shnirman, and G. Schön for helpful discussions. This work was partially supported by Korea Science and Engineering Foundation.

\* Electronic address: scoh@mrm.kaist.ac.kr

<sup>1</sup> P.W. Shor, in *Proceedings of the 35th Annual Symposium*

on the Foundation of Computer Science, ed. by S. Goldwasser (IEEE Computer Society Press, Los Alamos, CA,

- 1994), p. 124.
- <sup>2</sup> L.K. Grover, Phys. Rev. Lett. **79**, 325 (1997).
  - <sup>3</sup> P.W. Shor, Phys. Rev. A **52**, R2493 (1995).
  - <sup>4</sup> A.M. Steane, Phys. Rev. Lett. **77**, 793 (1996).
  - <sup>5</sup> J.I. Cirac and P. Zoller, Phys. Rev. Lett. **74**, 4091 (1995).
  - <sup>6</sup> C. Monroe, D.M. Meekhof, B.E. King, W.M. Itano, and D.J. Wineland, Phys. Rev. Lett. **75**, 4714 (1995).
  - <sup>7</sup> Q.A. Turchette, C.J. Hood, W. Lange, H. Mabuchi, and H.J. Kimble, Phys. Rev. Lett. **75**, 4710 (1995).
  - <sup>8</sup> I.L. Chuang, N. Gershenfeld, and M. Kubinec, Phys. Rev. Lett. **80**, 3408 (1998).
  - <sup>9</sup> D.G. Cory, M.D. Price, W. Maas, E. Knill, R. Laflamme, W.H. Zurek, T.F. Havel, and S.S. Somaroo, Phys. Rev. Lett. **81**, 2152 (1998).
  - <sup>10</sup> J.A. Jones, M. Mosca, and R.H. Hansen, Nature **393** 344 (1998).
  - <sup>11</sup> D. Loss and D.P. DiVincenzo, Phys. Rev. A **57** 120 (1998).
  - <sup>12</sup> B.E. Kane, Nature **393**, 133 (1998).
  - <sup>13</sup> J.E. Mooij, T. Orlando, L. Levitov, L. Tian, C. van der Wal, and S. Lloyd, Science **285**, 1036 (1999).
  - <sup>14</sup> A. Shnirman, G. Schön, and Z. Hermon, Phys. Rev. Lett. **79** 2371 (1997).
  - <sup>15</sup> D.V. Averin, Solid State Commun. **105**, 659 (1998).
  - <sup>16</sup> Y. Makhlin, G. Schön, and A. Shnirman, Nature **398**, 305 (1999).
  - <sup>17</sup> A. Shnirman and G. Schön, Phys. Rev. B **57**, 15 400 (1998).
  - <sup>18</sup> Y. Makhlin, G. Schön, and A. Shnirman, Rev. Mod. Phys. **73**, 357 (2001).
  - <sup>19</sup> R. Fazio, G.M. Palma, and J. Siewert, Phys. Rev. Lett. **83**, 5385 (1999).
  - <sup>20</sup> Y. Nakamura, Y.A. Pashkin, and J.S. Tsai, Nature **398**, 786 (1999).
  - <sup>21</sup> L. Dreher, Dipl. thesis. (Universität Karlsruhe, Karlsruhe, 1999); In this thesis only one value  $E_L = \sqrt{399}E_J$  is presented.
  - <sup>22</sup> W.H. Press, S.A. Teukolsky, W.T. Vetterling, and B.P. Flannery, *Numerical Recipes in C* (Cambridge University Press, New York, 1992) 2nd ed.
  - <sup>23</sup> C.P. Slichter, Principles of Magnetic Resonance, (Springer-Verlag, New York, 1992) 3rd ed. p623.
  - <sup>24</sup> J.F. Poyatos, J.I. Cirac, and P. Zoller, Phys. Rev. Lett. **78**, 390 (1997).